

Identifiability and Improvement of Adjoint Error Approach for Serial Robot Calibration[†]

Cheng Li¹, Yuanqing Wu¹, and Zexiang Li¹

Abstract—In this paper, we first analyze the identifiability of POE based Adjoint error approach. By carefully examining the linear dependence between calibration Jacobian columns, it is proved that joint offsets and Adjoint errors cannot be identified simultaneously, and the maximum dimension of identifiable parameters is $4r + 2t + 6$. Some more scenarios are considered to augment the Adjoint error approach. To satisfy the constraints on joint relations, constrained method and projection method are proposed. Moreover, we present the identifiability of reduction ratios and joint pitches. Simulations of a 6 Degree-of-Freedom robot and a SCARA robot are given to illustrate and compare our methods. It shows that the constrained method can handle such situations effectively and yields better results.

I. INTRODUCTION

The advancement of technology makes more and more robots serving for factory automation, especially in computer/communication/consumer electronics (3C) industry with higher demands on precision, efficiency and adaptation. Off-line programming is often used to quickly develop the robot-based automation system, and vision is now a regular tool for complex parts localization. Accuracy of the robot is of vital importance if a high precision of $0.03mm$ is expected in off-line programmed or visual guided motion. Kinematic calibration is an effective way to improve robot accuracy.

A good overview of calibration can be found in [1]. Generally speaking, a calibration process consists of 4 steps: modeling, measurement, identification and correction [2]. D-H convention [3] is widely used in modeling, with various modified versions such as Hayati model [4], complete and parametrically continuous (CPC) model [5] and so on. The product of exponentials (POE) formula is beginning to enter the mainstream of industrial robotics. Okamura and Park first employed POE model in calibration [6], based on which local POE model [7] and basic Adjoint error model [8] are derived. We propose a unified framework in [9] to summarize and compare these methods, which is a prequel to this paper. Some calibration examples can be found in [10]–[15].

Calibration models should satisfy the requirements of completeness, minimality and continuity [16]. Any redundancy should be eliminated. Using D-H or modified D-H

parameters, the maximum number of identifiable parameters is shown to be $4r + 2t + 6$ [17]–[19], where r is the number of revolute joints and t is the number of prismatic ones. Meggiolaro and Dubowsky analyzed the parameter redundancy in generalized error model and get the same result [20]. In POE based model, it is proven that joint offset errors are not identifiable in [8], but no analysis on its identifiability is presented. He *et al.* claim that the maximum number of identifiable parameters is $6r + 3t + 6$ [21] in POE model. However, they overlook the fact that some update components are of no effect after imposing constant pitch and unit norm constraints. When arguing the identifiability by linear dependence between calibration Jacobian columns, few literatures exam the whole columns composed by multiple samples. Thanks to the well-structured calibration Jacobian matrix in [9], we'll give the first careful analysis to show the maximum number of identifiable parameters is $4r + 2t + 6$ in POE model.

Beside the basic kinematics model, more facts should be taken into consideration. In addition to the constant pitch and unit norm constraints on a single joint, other constraints on joint relations are also important. For instance we may want two consecutive joints to keep parallel. Reasons are twofold. On the one hand, some relations are quite accurate comparing with the end-effector measurements. Since we cannot remove the noise out of measurement data, with such assumptions it is of more information and supposed to get a better result. On the other hand, in most commercial control systems certain joint relations are assumed and users have no way to change it. But to the authors' knowledge there are no previous works on dealing with such constraints in POE-based model. What's more, reduction ratios also need to be carefully treated. In many cases, RV or harmonic reducers are used and reduction ratios are exactly the ratios of gears' teeth number. However, in some other cases, reduction ratios are determined by the pitches of ball screws which may not be precise. Furthermore, when a ball screw with imprecise pitch is used as robot joint directly, which usually happens in SCARA robots, pitch becomes one joint coordinate that needs calibration. We will show that these variations are closely related to calibration basis and can be handled well.

This paper is organized as following: In section II we discuss the calibration identifiability, and prove the maximum dimension of identifiable parameters is $4r + 2t + 6$. Section III proposes methods to cope with constraints on joint relations. The way to incorporate reduction ratios and pitches is presented in section IV. In section V we conclude the paper and talk about possible future work.

[†]This project is supported by RGC Grant No.616509, No.615610 and No.615212; National Basic Research Program of China (973 Program, Grant No.2011CB013104); Key Joint Project of National Natural Science Foundation of China (Grant No.U1134004); Shenzhen Municipal Science and Technology Planning Program for Basic Research No. JCYJ20120618150931822; National Natural Science Foundation Grant No.51375413.

¹Department of Electronic and Computer Engineering, Hong Kong University of Science and Technology, Clear Water Bay, Kowloon, Hong Kong {cliac, eetroywu, eezxli}@ust.hk

II. IDENTIFIABILITY OF PARAMETERS

In [9], Adjoint error model and the calibration method are presented. The forward kinematics for a POE-based serial robot model is

$$g = e^{\hat{\xi}_1 \theta_1} e^{\hat{\xi}_2 \theta_2} \dots e^{\hat{\xi}_n \theta_n} e^{\hat{\Gamma}} \quad (1)$$

Subscript is used to denote joint number, and superscript for the number of sample. Totally m samples are measured. We follow the notation in [22] and further denote:

$$Ad_i^j = Ad_{e^{\hat{\xi}_i \theta_i^j}} \quad (2a)$$

$$Ad_0^i \triangleq I \quad (2b)$$

$$l_i = \left[\left(\prod_{k=0}^{i-1} Ad_k^1 \right)^T, \dots, \left(\prod_{k=0}^{i-1} Ad_k^m \right)^T \right]^T \xi_i \quad (2c)$$

$$Q_i = \begin{bmatrix} \prod_{k=0}^{i-1} Ad_k^1 - \prod_{k=0}^i Ad_k^1 \\ \vdots \\ \prod_{k=0}^{i-1} Ad_k^m - \prod_{k=0}^i Ad_k^m \end{bmatrix} \quad (2d)$$

$$Q_\Gamma = \left[\left(\prod_{k=0}^n Ad_k^1 \right)^T, \dots, \left(\prod_{k=0}^n Ad_k^m \right)^T \right]^T \quad (2e)$$

The Adjoint error of ξ_i is $\delta\eta_i$, and the Jacobian matrix A_{all} for all possible error parameters p_{all} is

$$A_{all} = [l_1, \dots, l_n, Q_1, \dots, Q_n, Q_\Gamma] \quad (3)$$

with

$$p_{all} = [\delta\theta_1, \dots, \delta\theta_n, \delta\eta_1^T, \dots, \delta\eta_n^T, \delta\eta_\Gamma^T]^T \quad (4)$$

$$y = \begin{bmatrix} (\delta g^1 \cdot (g^1)^{-1})^\vee \\ \vdots \\ (\delta g^m \cdot (g^m)^{-1})^\vee \end{bmatrix} = A_{all} \cdot p_{all} \quad (5)$$

where \vee extracts the vector from a skew-symmetric matrix.

If a column of A_{all} is linearly dependent on other columns, its corresponding parameter is not identifiable. We'll first prove that all joint offsets and Adjoint errors cannot be identified simultaneously, then find the maximum number of identifiable parameters, which is $rank(A_{all})$.

A. identifiability of joint offsets

If there exists a constant vector $c = [c_i^T, \dots, c_n^T, c_\Gamma^T]^T$ such that

$$l_i = [Q_i, \dots, Q_n, Q_\Gamma] \cdot c \quad (6)$$

then l_i and $[Q_i, \dots, Q_n, Q_\Gamma]$ are linearly dependent. Since A_{all} is well-structured, let $c_i = \dots = c_n = c_\Gamma = \xi_i$,

$$\begin{aligned} & [Q_i, \dots, Q_n, Q_\Gamma] \cdot c \\ &= (Q_i + \dots + Q_n + Q_\Gamma) \cdot \xi_i \\ &= \left[\left(\prod_{k=0}^{i-1} Ad_k^1 \right)^T, \dots, \left(\prod_{k=0}^{i-1} Ad_k^m \right)^T \right]^T \xi_i \\ &= l_i \quad (i = 1, 2, \dots, n) \end{aligned} \quad (7)$$

Therefore, for any joint, its offset is always linearly dependent on Adjoint errors. In other words, we can never calibrate joint offsets and Adjoint errors at the same time. Physically it means that end-effector error caused by joint offsets can always be equivalently treated as that caused by Adjoint errors, as shown in Fig.1.

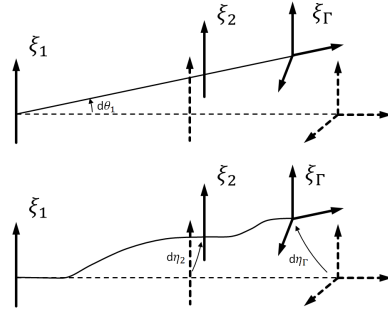


Fig. 1. End-effector error caused by joint offset or Adjoint errors

Such redundancy should be eliminated. We can simply assume that the error of end-effector comes only from Adjoint errors without any joint offsets, in which case

$$A = [Q_1, \dots, Q_n, Q_\Gamma] \quad (8)$$

$$p = [\delta\eta_1^T, \dots, \delta\eta_n^T, \delta\eta_\Gamma^T]^T \quad (9)$$

Now p has $6n + 6$ parameters.

B. rank of calibration Jacobian matrix

We analyze $rank(A)$ by finding out the kernel $ker(A)$. From [9] we get the following lemma.

Lemma 1: $\mathfrak{c}(\xi)$ and $\mathfrak{r}(\xi)$ are the cylindrical and schönflies lie subalgebra associated with joint ξ . When $\xi = [v^T, \omega^T]^T$ is not a prismatic joint,

$$ker(I - Ad_{e^{\hat{\xi}\theta}}) = \mathfrak{c}(\xi) \quad (10)$$

$$range(I - Ad_{e^{\hat{\xi}\theta}}) = \mathfrak{c}\left(\begin{bmatrix} \omega \\ v \end{bmatrix}\right)^\perp \quad (11)$$

When $\xi = [v^T, 0]^T$ is a prismatic joint,

$$ker(I - Ad_{e^{\hat{\xi}\theta}}) = \mathfrak{r}(\xi) \quad (12)$$

$$range(I - Ad_{e^{\hat{\xi}\theta}}) = \mathfrak{r}\left(\begin{bmatrix} 0 \\ v \end{bmatrix}\right)^\perp \quad (13)$$

Corollary 1: $\xi \notin range(I - Ad_{e^{\hat{\xi}\theta}})$

It is easy to see that each Q_i contributes a kernel part

$$\mathcal{N}_i = span\{[\dots, 0, \zeta_i^T, 0, \dots]^T\} \quad (14)$$

where $\zeta_i \in ker(I - Ad_{e^{\hat{\xi}_i \theta_i}})$. By the lemma, $Dim(\mathcal{N}_i) = 4$ if ξ_i is a prismatic joint, $Dim(\mathcal{N}_i) = 2$ if not. The whole kernel \mathcal{N} contains at least the direct sum of each \mathcal{N}_i

$$\mathcal{N} \supseteq \mathcal{N}_s = \bigoplus \mathcal{N}_i \quad (15)$$

So $Dim(\mathcal{N}) \geq Dim(\mathcal{N}_s) = 2r + 4t$, leaving at most $4r + 2t + 6$ parameters to be identifiable. We'll prove next that $\mathcal{N} = \mathcal{N}_s$ if samples are taken properly.

For a serial robot with n joints, we take $2n$ samples:

$$\begin{cases} \theta^{2i-1} = [0, \dots, 0, \theta_i^{2i-1}, 0, \dots, 0] \\ \theta^{2i} = [0, \dots, 0, \theta_i^{2i}, 0, \dots, 0] \end{cases} \quad (16)$$

where $\theta_i^{2i-1} \neq \theta_i^{2i}$, $\theta_i^{2i-1} \neq 0$, $\theta_i^{2i} \neq 0$. The sample strategy is to take two different non-zero angles each time joint by joint. The calibration Jacobian matrix becomes

$$A = \begin{bmatrix} I - Ad_1^1 & \dots & 0 & Ad_1^1 \\ I - Ad_1^2 & \dots & 0 & Ad_1^2 \\ \vdots & \ddots & \vdots & \vdots \\ 0 & \dots & I - Ad_n^{2n-1} & Ad_n^{2n-1} \\ 0 & \dots & I - Ad_n^{2n} & Ad_n^{2n} \end{bmatrix} \quad (17)$$

TABLE I
PARAMETER OF 6 DOF ROBOT (UNIT:MM)

	Nominal	Strict	Relax
ξ_1	(0,0,0,0,1)	(0,0,0,-0.0069,0.0110,0.9999)	(0,0,0,-0.0069,0.0110,0.9999)
ξ_2	(-450,0,150,0,1,0)	(-456.2702,7.1714,153.1302,0.0120,0.9998,-0.0109)	(-456.2685,7.1912,153.1345,0.0121,0.9999,-0.0110)
ξ_3	(-1020,0,150,0,1,0)	(-1027.0507,14.7527,217.8679,0.0120,0.9998,-0.0109)	(-1027.06126,14.7820,217.8160,0.0121,0.9999,-0.0110)
ξ_4	(0,1170,0,1,0,0)	(15.5054,1203.4094,-7.6911,0.9832,-0.0138,-0.1819)	(15.4571,1203.4096,-7.7516,0.9832,-0.0138,-0.1819)
ξ_5	(-1170,0,800,0,1,0)	(-1057.6017,-44.4919,873.1381,0.0301,0.9957,0.0872)	(-1057.5397,-44.5567,873.2099,0.0301,0.9957,0.0873)
ξ_6	(0,1170,0,1,0,0)	(21.0239,1161.2066,-12.4274,0.9922,-0.0193,-0.1228)	(20.9662,1161.2069,-12.4967,0.9922,-0.0192,-0.1228)
ξ_Γ	(850,0,1170,0,0,0)	(932.9693,3.1212,1067.1911,0,0,0)	(932.9693,3.1212,1067.1911,0,0,0)

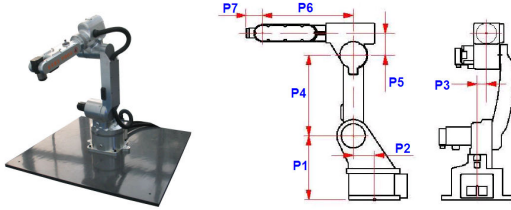


Fig. 3. A 6 DoF robot and its parameter definition

E. Example: 6 DoF robot

Robot and its parameter definition are shown in Fig. 3.

As you can see, parameters are of D-H style and the following joint relations are assumed at initial configuration:

- 1) joint 1 and 2 are perpendicular.
- 2) joint 2 and 3 are parallel.
- 3) joint 3 and 4 are perpendicular.
- 4) joint 4, 5, 6 are perpendicular to each other, and intersect at one point.

Three calibration methods are implemented and compared, namely "free method" that ignores all the constraints, "constrained method" that calibrates the robot under constraints by choosing proper basis, and "projection method" that projects the result of free method in each iteration.

Since all the joints are under certain perpendicular/parallel restrictions, we assign the $so(3)$ rotational change freedom to the whole robot, of which the basis is B_r . Joint offsets $\delta\theta_3$, $\delta\theta_4$ and $\delta\theta_5$ are introduced to handle perpendicular constraints. $\delta\theta_1$ is not needed because it is covered in B_r . Joint 1,2,3 have their own translational change B_{t_i} ($i = 1, 2, 3$), and the last three joints have the same translational basis B_{t_q} . The whole basis matrix is

$$B = \begin{bmatrix} I_3 & 0 & 0 & 0 & 0 & 0 & 0 \\ 0 & B_r & B_{t_1} & 0 & 0 & 0 & 0 \\ 0 & B_r & 0 & B_{t_2} & 0 & 0 & 0 \\ 0 & B_r & 0 & 0 & B_{t_3} & 0 & 0 \\ 0 & B_r & 0 & 0 & 0 & B_{t_q} & 0 \\ 0 & B_r & 0 & 0 & 0 & B_{t_q} & 0 \\ 0 & B_r & 0 & 0 & 0 & B_{t_q} & 0 \\ 0 & B_r & 0 & 0 & 0 & 0 & I_\Gamma \end{bmatrix} \quad (32)$$

where I_3 is the part for joint offsets, and I_Γ stands for the initial configuration error of tool frame.

Two sets of joint coordinates are generated and listed in Table I. In the "strict" model we carefully keep all constraints satisfied, while in "relax" model we perturb it a little bit. For example, there is a 0.023° difference for joint 1,2 to be perpendicular. 100 poses are picked randomly in workspace and end-effector configurations are measured for calibration. Gauss noise is added to each measurement with standard deviation $0.02mm$ in position components and standard deviation $0.0002rad$ in orientation components. Another 500

samples are randomly picked for verification. Error is the maximum distance of points $(0, 0, 0)$, $(100, 0, 0)$, $(0, 100, 0)$, $(0, 0, 100)$ (mm) in tool frame between actual and calibrated models. Calibration process is repeated for 1000 times and the error histograms is shown in Fig.4. Repeating the process and evaluating the methods' performance by histograms can eliminate the random factors and make the result comparable. In real application, we don't need to repeat.

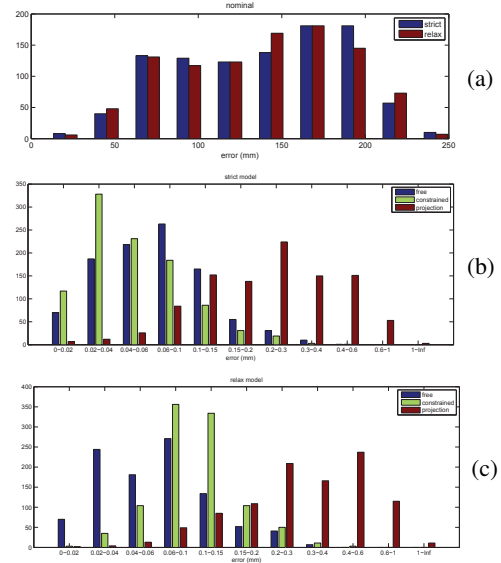


Fig. 4. 6 DoF Robot Simulation: error of (a) model with nominal parameters; (b) strict model; (c) relax model

Errors of nominal model are quite large due to the large kinematics error we introduced (about $5mm$ in length of links and 5° in joint offsets), and errors are reduced obviously after calibration. In strict model the constrained method is the best, while in relax model the free method is better than constrained method, in statistic sense. It is quite reasonable. When real joint relations satisfy the constraints, free method is driven away by measurement noises. But in relax model, constrained method cannot compensate errors away from nominal constraints. To our surprise, projection method is always the worst.

If we compare the same method between two models, the error levels of free method is close, showing the consistency of its performance; but constrained and projection method are much worse in relax model. Given that most commercial control systems do have the restriction, it's really important for real robot to satisfy the constraints as well as possible. One way to exam how well the constraints are satisfied is to compare the results of free and constrained methods.

TABLE II
PARAMETER OF SCARA ROBOT (UNIT:MM)

	Nominal	Strict	Relax
ξ_1	(0,0,0,0,1)	(0,0,0,-0.0459,-0.0576,0.9973)	(0,0,0,-0.0456,-0.0576,0.9973)
ξ_2	(0,-225,0,0,1)	(16.1511,-225.8596,-12.2966,-0.0459,-0.0576,0.9973)	(16.1687,-225.8598,-12.2701,-0.0459,-0.0575,0.9973)
ξ_3	(0,0,1,0,0,0)	(-0.0459,-0.0576,0.9973,0,0,0)	(-0.0458,-0.0576,0.9973,0,0,0)
ξ_4	(0,-350,16/(2 π),0,0,1)	(38.9140,-343.9504,-15.4992,-0.0459,-0.0576,0.9973)	(38.9016,-343.9506,-15.5249,-0.0458,-0.0576,0.9973)
ξ_Γ	(350,0,217,0,0,0)	(337.2009,27.3724,237.0478,0,0,0)	(337.2009,27.3724,237.0478,0,0,0)
r	(1/80, 1/50, 5/6, 1/11.4)	(1/80.2, 1/49.9, 0.85, 1/11.27)	

IV. REDUCTION RATIO AND PITCH

A. reduction ratio

Apart from the geometric parameters discussed above, reduction ratios may also need calibration. To be general, let's assume all reduction ratios are imprecise. The forward kinematics formula with reduction ratios is

$$f = e^{\hat{\xi}_1 r_1 \theta_1} e^{\hat{\xi}_2 r_2 \theta_2} \dots e^{\hat{\xi}_n r_n \theta_n} e^{\hat{\Gamma}} \quad (33)$$

Denote

$$Ad_i^j = Ad_{e^{\hat{\xi}_i r_i \theta_i^j}} \quad (34)$$

It should not be confused with the previous notation. After all, they are the same formula with or without reduction ratio being expressed explicitly. The calibration Jacobian column for reduction ratio error δr_i is

$$u_i = \left[\left(\prod_{k=0}^{i-1} Ad_k^1 \right)^T \theta_i^1, \dots, \left(\prod_{k=0}^{i-1} Ad_k^m \right)^T \theta_i^m \right]^T \xi_i \quad (35)$$

With reduction ratios, the calibration Jacobian now is

$$A_r = [u_1, \dots, u_n, Q_1, \dots, Q_n, Q_\Gamma] \quad (36)$$

with corresponding error vector

$$p_r = [\delta r_1, \dots, \delta r_n, \delta \eta_1^T, \dots, \delta \eta_n^T, \delta \eta_\Gamma^T]^T \quad (37)$$

$\ker(A_r) = \mathcal{N}_r$ is augmented from \mathcal{N}

$$\mathcal{N}_r = [0, \dots, 0]^T \times \mathcal{N} \quad (38)$$

Similar sample strategy and argument is used to get $\text{rank}(A_r)$. After matrix manipulation,

$$A'_r = \begin{bmatrix} \theta_1^1 \xi_1 & \dots & 0 & I - Ad_1^1 & \dots & 0 & I \\ \theta_2^1 \xi_2 & \dots & 0 & I - Ad_2^1 & \dots & 0 & I \\ \vdots & \ddots & \vdots & \vdots & \ddots & \vdots & \vdots \\ 0 & \dots & \theta_n^{2n-1} \xi_n & 0 & \dots & I - Ad_n^{2n-1} & I \\ 0 & \dots & \theta_n^{2n} \xi_n & 0 & \dots & I - Ad_n^{2n} & I \end{bmatrix} \quad (39)$$

We want to find $x_r = [y_1, \dots, y_n, x_1^T, \dots, x_n^T, x_\Gamma^T]^T \notin \mathcal{N}_r$ such that $A'_r x_r = 0$. Re-order the terms and we get

$$\begin{cases} (I - Ad_i^{2i-1})x_i + \xi_i \theta_i^{2i-1} y_i = -x_\Gamma \\ (I - Ad_i^{2i})x_i + \xi_i \theta_i^{2i} y_i = -x_\Gamma \end{cases} \quad (40)$$

If $x_\Gamma = 0$,

$$(I - Ad_i^{2i})x_i + \xi_i \theta_i^{2i} y_i = 0 \quad (41)$$

According to the corollary, $\xi \notin \text{range}(I - Ad_{e^{\hat{\xi}\theta}})$. So $x_i \in \ker(I - Ad_i^{2i})$, $y_i = 0$, then $x_r \in \mathcal{N}_r$.

If $x_\Gamma \neq 0$, subtract the two equations,

$$\begin{aligned} & (Ad_i^{2i-1} - Ad_i^{2i})x_i + \xi_i (\theta_i^{2i-1} - \theta_i^{2i}) y_i \\ & = Ad_i^{2i-1} (I - Ad_{e^{\hat{\xi}_i (\theta_i^{2i-1} - \theta_i^{2i})}}) x_i + \xi_i (\theta_i^{2i-1} - \theta_i^{2i}) y_i \\ & = 0 \end{aligned} \quad (42)$$

Since $\theta_i^{2i-1} \neq \theta_i^{2i}$, the same argument holds, so

$$\begin{cases} x_i \in \ker(I - Ad_{e^{\hat{\xi}_i (\theta_i^{2i-1} - \theta_i^{2i})}}) = \ker(I - Ad_i^{2i}) \\ y_i = 0 \end{cases} \quad (43)$$

which conflicts the fact $(I - Ad_i^{2i})x_i + \xi_i \theta_i^{2i} y_i = -x_\Gamma \neq 0$. Therefore no such x_r can be found, which proves that \mathcal{N}_r is all the kernel, and reduction ratios can be calibrated.

Although there's one more identifiable parameters associated with each joint, strictly speaking reduction ratio is not a geometric parameter. The maximum dimension of identifiable geometric parameters is still $4r + 2t + 6$.

B. pitch

In Adjoint error model the joint pitch keeps unchanged in calibration. It is useful for zero and infinite pitch joints. But what about a finite pitch joint with imprecise pitch? We can go back to Park's scheme [6], but at the same time we get back the unit norm constraint. After knowing the way to deal with joint relation constraints and reduction ratios, instead of one joint ξ_h with imprecise pitch, we can decompose it to a revolute joint ξ_r coincided with a prismatic one ξ_t . The angles are related by the pitch h .

$$\xi_h = \begin{bmatrix} -\omega \times q + h\omega \\ \omega \end{bmatrix}, \xi_r = \begin{bmatrix} -\omega \times q \\ \omega \end{bmatrix}, \xi_t = \begin{bmatrix} \omega \\ 0 \end{bmatrix} \quad (44)$$

$$e^{\hat{\xi}_h r \theta} = e^{\hat{\xi}_r r \theta} e^{\hat{\xi}_t h r \theta} = e^{\hat{\xi}_t h r \theta} e^{\hat{\xi}_r r \theta} \quad (45)$$

So the problem is converted to the one we can solve. An example of SCARA robot is presented next to illustrate how to deal with reduction ratios and pitches.

C. Example: SCARA

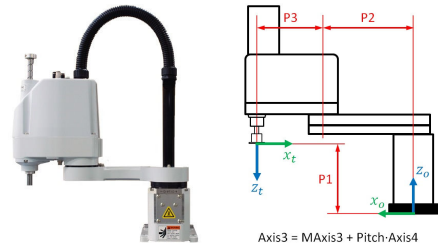


Fig. 5. A SCARA robot and its parameter definition

Fig.5 shows the robot and its parameter definition. Joint coordinates of strict model and relax model are listed in Table II. The last line contains reduction ratios. Joint 4 is decomposed and the equivalent forward kinematics is

$$f = e^{\hat{\xi}_1 r_1 \theta_1} e^{\hat{\xi}_2 r_2 \theta_2} e^{\hat{\xi}_3 (r_3 \theta_3 + h r_4 \theta_4)} e^{\hat{\xi}_4 r_4 \theta_4} e^{\hat{\Gamma}} \quad (46)$$

where ξ'_4 is the rotational part of ξ_4 . It is not hard to write out its calibration basis.

$$B = \begin{bmatrix} I_5 & 0 & 0 & 0 & 0 & 0 \\ 0 & B_r & B_{t1} & 0 & 0 & 0 \\ 0 & B_r & 0 & B_{t2} & 0 & 0 \\ 0 & B_r & 0 & 0 & 0 & 0 \\ 0 & B_r & 0 & 0 & B_{t4} & 0 \\ 0 & B_r & 0 & 0 & 0 & I_\Gamma \end{bmatrix} \quad (47)$$

I_5 is the block for pitch and reduction ratios. Same sample strategy and verification method are used as in the previous simulation, and error histograms are shown in Fig.6.

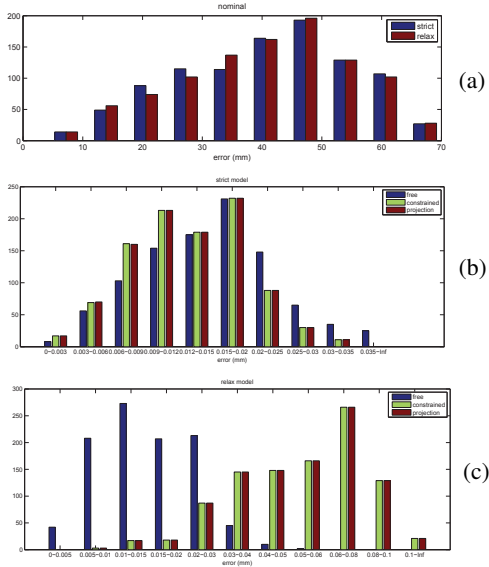


Fig. 6. SCARA Robot Simulation: error of (a) model with nominal parameters; (b) strict model; (c) relax model

In this simulation, errors are also reduced significantly by calibration. Performances of constrained and projection method are nearly the same. That may because SCARA's constraints are relatively simple. This simulation illustrates that reduction ratios and pitches can be identified by our calibration approach.

V. CONCLUSION AND FUTURE WORK

In this paper, by examining the rank of calibration Jacobian matrix, we first prove that the maximum dimension of identifiable parameters is $4r + 2t + 6$ in POE model. Since real robots and control systems are concerned, we then propose constrained method and projection method to handle constraints on joint relations. Moreover, calibration of reduction ratios and pitched can also be handled well by augmenting the error basis, and its identifiability is proved. Simulations on a 6 DoF robot and a SCARA robot are presented to illustrate and compare the performance. Real experiments are under preparation to verify the effectiveness of our calibration methods.

In our simulations, random samples are taken over the robots workspace. In literatures the sample strategy can be optimized by maximizing observation index, mostly in numerical or heuristic methods. Analytical relation is hard to find due to the complicated calibration Jacobian structure. In Adjoint error model the structure is quite simple and clear. One possible future work is to find the analytical relation thus optimization could be easy and efficient.

REFERENCES

- [1] J.M. Hollerbach and C.W. Wampler. The calibration index and taxonomy for robot kinematic calibration methods. *The international journal of robotics research*, 15(6):573–591, 1996.
- [2] Z. Roth, B. Mooring, and B. Ravani. An overview of robot calibration. *Robotics and Automation, IEEE Journal of*, 3(5):377–385, 1987.
- [3] R.P. Paul. *Robot manipulators: mathematics, programming, and control: the computer control of robot manipulators*. Richard Paul, 1981.
- [4] S.A. Hayati. Robot arm geometric link parameter estimation. In *Decision and Control, 1983. The 22nd IEEE Conference on*, volume 22, pages 1477–1483. IEEE, 1983.
- [5] H.Q. Zhuang, Z. Roth, and F. Hamano. A complete and parametrically continuous kinematic model for robot manipulators. *Robotics and Automation, IEEE Transactions on*, 8(4):451–463, 1992.
- [6] K. Okamura and F.C. Park. Kinematic calibration using the product of exponentials formula. *Robotica*, 14(4):415–422, 1996.
- [7] I. Chen, G.L. Yang, C.T. Tan, and S.H. Yeo. Local poe model for robot kinematic calibration. *Mechanism and Machine Theory*, 36(11):1215–1239, 2001.
- [8] Y.J. Lou, T.N. Chen, Y.Q. Wu, Z.B. Li, and S.L. Jiang. Improved and modified geometric formulation of poe based kinematic calibration of serial robots. In *Intelligent Robots and Systems, 2009. IROS 2009. IEEE/RSJ International Conference on*, pages 5261–5266. IEEE, 2009.
- [9] Y.Q. Wu, C. Li, J. Li, and Z. Li. Comparative study of robot kinematic calibration algorithms using a unified geometric framework. In *Robotics and Automation, 2014. Proceedings 2014 ICRA. IEEE International Conference*. IEEE.
- [10] A. Nubiola and I.A. Bonev. Absolute calibration of an abb irb 1600 robot using a laser tracker. *Robotics and Computer-Integrated Manufacturing*, 2012.
- [11] A. Omodei, G. Legnani, and R. Adamini. Three methodologies for the calibration of industrial manipulators: experimental results on a scara robot. *Journal of Robotic Systems*, 17(6):291–307, 2000.
- [12] P. Rousseau, A. Desrochers, and N. Krouglicof. Machine vision system for the automatic identification of robot kinematic parameters. *Robotics and Automation, IEEE Transactions on*, 17(6):972–978, 2001.
- [13] C.H. Gong, J.X. Yuan, and J. Ni. A self-calibration method for robotic measurement system. *Journal of manufacturing science and engineering*, 122(1):174–181, 2000.
- [14] M. Ikits and J.M. Hollerbach. Kinematic calibration using a plane constraint. In *Robotics and Automation, 1997. Proceedings., 1997 IEEE International Conference on*, volume 4, pages 3191–3196. IEEE, 1997.
- [15] M.A. Meggiolaro, G. Scriffignano, and S. Dubowsky. Manipulator calibration using a single endpoint contact constraint. In *Proceedings of ASME Design Engineering Technical Conference, Baltimore, USA, 2000*.
- [16] K. Schröder, S.L. Albright, and M. Grethlein. Complete, minimal and model-continuous kinematic models for robot calibration. *Robotics and Computer-Integrated Manufacturing*, 13(1):73–85, 1997.
- [17] L.J. Everett and A.H. Suryohadiprojo. A study of kinematic models for forward calibration of manipulators. In *Robotics and Automation, 1988. Proceedings., 1988 IEEE International Conference on*, pages 798–800. IEEE, 1988.
- [18] L.J. Everett and H. TSING-WONG. The theory of kinematic parameter identification for industrial robots. *Journal of dynamic systems, measurement, and control*, 110(1):96–100, 1988.
- [19] W. Khalil, M. Gautier, and Ch. Enguehard. Identifiable parameters and optimum configurations for robots calibration. *Robotica*, 9(01):63–70, 1991.
- [20] M.A. Meggiolaro and S. Dubowsky. An analytical method to eliminate the redundant parameters in robot calibration. In *Robotics and Automation, 2000. Proceedings. ICRA'00. IEEE International Conference on*, volume 4, pages 3609–3615. IEEE, 2000.
- [21] R.B. He, Y.J. Zhao, S.N. Yang, and S.Z. Yang. Kinematic-parameter identification for serial-robot calibration based on poe formula. *Robotics, IEEE Transactions on*, 26(3):411–423, 2010.
- [22] Z. Li, S.S. Sastry, and R.M. Murray. A mathematical introduction to robotic manipulation, 1994.